LOCALIZING IMPEDANCE SOURCES FROM BETATRON PHASE BEATING IN THE CERN SPS

G. Arduini, C. Carli, F. Zimmermann, CERN, Geneva, Switzerland

Abstract

Multi-turn beam-position data recorded after beam excitation can be used to extract the betatron-phase advance between adjacent beam position monitors (BPMs) by a harmonic analysis. Performing this treatment for different beam intensities yields the change in phase advance with current. A local impedance contributes to the average tune shift with current, but it also causes a mismatch and phase beating. We describe an attempt to determine the localized impedance around the SPS ring by fitting the measured betatron phase shift with current at all BPMs to the expected impedance response matrix.

INTRODUCTION

In 2003, the SPS transverse impedance, as deduced from the coherent tune shift with current, increased by about 50% [1] with respect to the previous year. This increase was tentatively attributed to the (re-)installation of 5 modified ferrite kickers in the 2002/03 shutdown, and it was consistent with an analytical estimate [2].

However, the theoretical uncertainties appear not negligible, and a direct beam-based localization of the largest impedance sources in the SPS — and later in the LHC — would be highly desirable. One possible method to measure the impedance locally around the ring is to detect the current-dependent phase advance between adjacent BPMs. At LEP such a method was applied successfully [3], confirming that the rf cavities in the straight sections were the dominant sources of transverse impedance. It was sufficient to compute the accumulated phase advance around the ring, which monotonically decreased with beam current and declined more steeply at the high-impedance sections. In the SPS the same type of analysis was attempted in 2000/2001 [4], but the error bars were large and no definite conclusion could be drawn.

Recently we recognized that localized impedance sources do not only introduce a step in the accumulated phase advance around the machine, but they also induce a phase beating. At LEP the beating was small, since the rf cavities extended over several optical cells. In the SPS, the kickers are localized within part of a single cell, and the beating could be a large effect. We here report on an attempt to extract the local impedance distribution around the SPS ring from the measured current-dependent phase beating.

The procedure for measuring the betatron phase from a turn-by-turn beam-position monitor reading was also developed at LEP [5]. The oscillation at the kth BPM on turn m be $x_{km} = A_k \cos(2\pi m Q_x + \phi_{0,k})$, with A_k the measured amplitude. If x_{km} is recorded over many turns $N \gg 1$, the betatron phase at the kth BPM is [5] $\phi_{0,k} \approx -\arctan(S_k/C_k)$, where $C_k = \sum_{m=1}^{N} x_{km} \cos(2\pi m Q_x)$, and $S_k = \sum_{m=1}^{N} x_{km} \sin(2\pi m Q_x)$. Differences in the phase advances $(\phi_{0,k} - \phi_{0,k-1})$ at different beam currents contain information on the localized transverse impedance.

OPTICS PERTURBATION

Considering one plane only, e.g., the vertical, and a Gaussian bunch profile, the impedance acts like a current dependent quadrupole of effective gradient

$$K_{\rm eff} = -\frac{N_b e}{2\sqrt{\pi}\sigma_z (E_b/e)} {\rm Im} Z_{\perp,{\rm eff}} \ , \qquad (1)$$

where N_b denotes the bunch population and $Z_{\perp,{\rm eff}}$ the effective impedance, e.g., in this case, the impedance weighted with the bunch power spectrum [6]. Note that the vertical impedance acts always defocusing.

A focusing change of strength ΔK at location s_0 introduces a tune change and a phase beating. In first order, the tune change is $\Delta Q = \beta_k \Delta K/(4\pi)$, and the phase beating

$$\Delta\phi(s) = \begin{cases} \left[\frac{\beta_k \cos(\phi(s) - 2\phi_k + 2\pi Q_0)\sin\phi(s)}{2\sin(2\pi Q_0)}\right]\Delta K \\ \text{for } \ \phi({\rm s}) < \phi_{\rm k} \\ \left[\frac{\beta_k}{2} - \frac{\beta_k \cos(\phi(s) - 2\phi_k)\sin(\phi(s) - 2\pi Q_0)}{2\sin(2\pi Q_0)}\right]\Delta K \\ \text{for } \ \phi({\rm s}) > \phi_{\rm k} \end{cases} , \qquad (2)$$

where β_k denotes the beta function at s_0. Applying (2) to the gradient errors ΔK of all quadrupoles, the associated phase changes $\Delta\phi$ at the BPM locations can be expressed, more succinctly, in vector notation as

$$\Delta\vec{\phi} = M\Delta\vec{K} \ . \qquad (3)$$

The matrix M is computed from the SPS optics model in MAD. If $\Delta\vec{\phi}$ is measured, we can then solve for the vector $\Delta\vec{K}$ of effective quadrupole-gradient errors around the ring, using a standard minimization procedure, such as Micado or singular-value decomposition (SVD). The SVD solution needs to be stabilized by constraining the magnitude of the quadrupole changes $\Delta\vec{K}$. This is done by including a set of additional equations of the form

$$\lambda\Delta\vec{K} = 0 \ , \qquad (4)$$

and solving the combined system of equations (3) and (4). By adjusting the weight λ and also, possibly, the cut-off for singular values in the inversion of the SVD diagonal matrix, the solution can be optimized.

Associated with the phase beating is a beta beating,

$$\Delta\beta(s) = -\frac{\beta(s)\beta_k \cos(2|\phi(s) - \phi_k| - 2\pi Q)}{2\sin(2\pi Q)}\Delta K \ . \qquad (5)$$

This equation could be included in the minimization, but unlike the phases, the local beta function inferred from the 1000-turn measurement is sensitive to the calibration and scale errors of the beam-position monitors, which might be current dependent.

The equation system (3) describes the effect of the impedance, if we replace $\Delta\vec{\phi}$ on the left with $\Delta\vec{\phi}/\Delta N_b$, and $\Delta\vec{K}$ on the right by a current-dependent focusing term $\Delta\vec{K}_{\rm eff}/\Delta N_b$. The elements in the response matrix M of (3) are the same as those given on the right-hand side of (2) for the effect of quadrupole-strength changes.

TESTS OF THE ALGORITHM

We verified that our algorithm can identify the location of a quadrupole-gradient change, by varying the strength of a single quadrupole (QE603) in MAD and taking the resulting phase changes at all BPMs as input. The correct quadrupole is identified either by determining the best single quadrupole change or by performing a pseudo-inversion by SVD. Since we use a linearized 1st order description of the phase beating, the agreement between actual and fitted quadrupole strengths becomes worse as the gradient change is increased. For an associated tune change of 0.1 the error in the quadrupole strength is about 5%; for a tune change of less than 0.01, the error stays below 0.3%. In this case the nonlinear terms should not be a concern.

The procedure outlined above can only function if the MAD optics model is sufficiently close to the real optics. To explore the efficiency and reliability of our method in practice, we performed an experimental test, where we recorded 1000-turn BPM data before and after varying the strength of the same single quadrupole by -0.0061 m^{-1}, corresponding to $\Delta Q \approx -0.05$. Figure 1 shows example results from the SVD solution. They illustrate the importance of the correct choice of λ. If λ is too small (left side), a perfect fit to the model optics is obtained, but one which requires large excitation of many quadrupoles all around the machine. If λ is too large (right side), the fit becomes poor. In an intermediate range $\lambda \approx 50 - 100$ (centre) the fit looks reasonable and the largest quadrupole-gradient change is found at the correct location — actually for the neighboring magnet QD603, presumably due to small differences between the MAD model and the real optics, and due to the thin-lens approximation on which our response matrix (2) is based.

Alternatively we determined the most efficient single 'corrector' for minimizing the quality function Q, $1/Q \equiv \min_{\phi_c} \sum(\phi_{\rm fit} - \phi_{\rm meas} - \phi_c)^2/\sigma_\phi^2$, with σ_ϕ the error of the phase measurement and ϕ_c a constant offset between measurement and model. In this case, the correct quadrupole $QE603$ is identified with a fitted strength change of -0.65 m^{-1}, i.e., 6% larger than the actual change.

IMPEDANCE LOCALIZATION

Two experiments were performed at 26 GeV/c, on 04.09. and 30.09.03, and one experiment at 14 GeV/c, on 27.10.03. In each experiment, the beam was kicked transversely and 1000-turn readings were recorded for all ring BPMs. The intensity of a single proton bunch was varied in 4–6 steps, between about 2×10^{10} and 1.2×10^{11}. Chromaticity was held at the lowest value compatible with beam stability. Increasing the longitudinal emittance allowed reducing the chromaticity and improved the data quality. Some example BPM readings for high and low intensity at 26 GeV/c and 14 GeV/c are shown in Fig. 2. We observe that the decoherence time and, at 14 GeV/c, also the closed orbit vary with beam intensity.

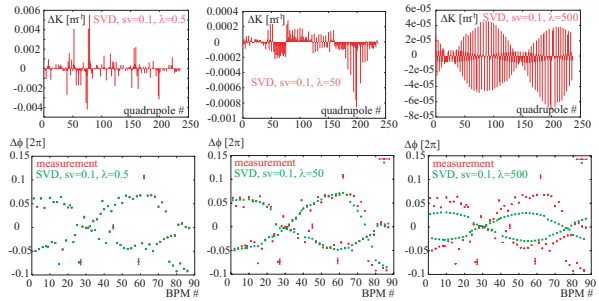

Figure 1: Top row: quadrupole gradients obtained by fitting the measured phase change at the BPMs by SVD inversion with an SVD eigenvalue cut-off parameter of 0.1 and three different weights λ as indicated. Bottom row: the corresponding fit result superimposed on the measurement.

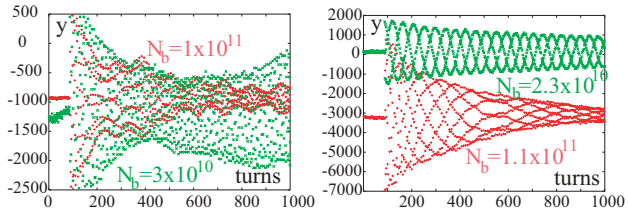

Figure 2: Vertical position in arb. units vs. turn number at 26 Gev/c (left) and 14 GeV/c (right); in either case, typical signals for high and low bunch intensity are displayed.

For each data set, we compute the average tune over all BPMs as well as the rms tune spread. In Fig. 3, the tune is displayed as a function of bunch intensity. Data sets with large tune error are discarded in the harmonic analysis, since a large variation of the tune from BPM to BPM implies a large uncertainty in the phase.

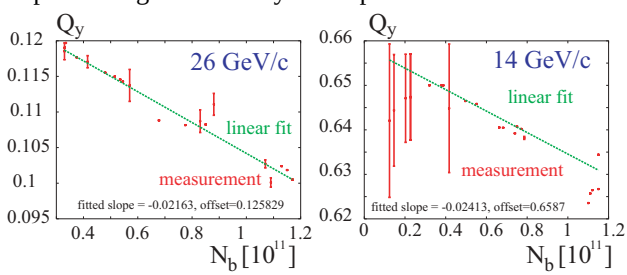

Figure 3: Vertical tune averaged over all BPM readings vs. bunch intensity at 26 Gev/c (left) and 14 GeV/c (right); the error bar indicates the spread between BPMs.

The analysis of the good data sets proceeds as follows. We determine the phase of betatron oscillation with respect to the start of the line for each BPM and each data set. Since the phase is not uniquely defined we constrain it to lie within $\pm\pi$ of the MAD model phase.

For each BPM we fit the dependence of the betatron phase on the bunch intensity to a linear relation as

$$\phi_\beta = \phi_0 + (\Delta\phi/\Delta N_b)\, N_b \,. \qquad (6)$$

The offset ϕ_0 characterizes the optics phase error at zero beam intensity and the slope $\Delta\phi/\Delta N_b$ the effect of the impedance. In Fig. 4 the quantity $\Delta\phi \equiv (\phi_\beta - \phi_0)$ is displayed as a function of the intensity together with the linear fit (6), for a few BPMs from different regions of the SPS. The variation with intensity is linear within the fluctuation of the measurement. The data at 14 GeV/c are less noisy.

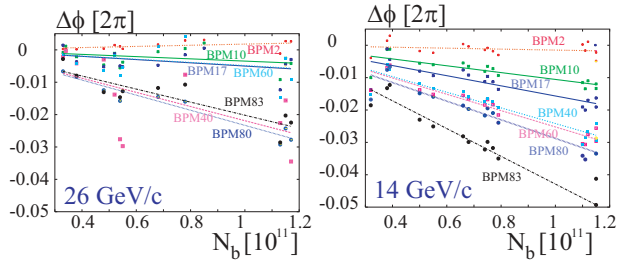

Figure 4: Measured phase variation $\Delta\phi$ vs. bunch intensity for 7 selected BPMs together with the linear fit (6), at 26 Gev/c (left) and 14 GeV/c (right).

Figure 5 shows the two fit variables ϕ_0 and $\Delta\phi/\Delta N_b$, including error bars from the fit, for all BPMs, at 26 GeV/c and 14 GeV/c. On the left, the monotonic increase in offset ϕ_0 with BPM number up to a value of 0.08 (2π) at 14 GeV/c is explained by the difference between the model tune 26.579 and the fitted zero-current tune of 26.659 (see Fig. 3). In the right picture, the phase shift with current $|\Delta\phi/\Delta N_b|$ increases similarly around the ring at the two beam energies; the increase is larger for the lower energy, as expected from (1). The data for 14 GeV/c clearly reveal a beating pattern superimposed on a gradual decline. At 26 GeV/c the beating is less evident.

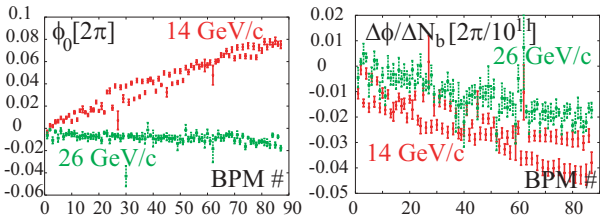

Figure 5: Fitted zero-current betatron phase error (left) and the phase shift with bunch intensity (right) at 26 GeV/c and 14 GeV/c.

For simplicity, we consider potential impedance sources at the positions of the 237 quadrupole magnets, so that the matrix M is identical to the quadrupole-response matrix employed above when testing the algorithm. Similar to the procedure for a real quadrupole variation, the impedance-related focusing-strength changes $\Delta\vec{K}_{\rm eff}/\Delta N_b$ are calculated from the fitted phase slopes $\Delta\vec{\phi}/\Delta N_b$, by means of an SVD fit, including the additional constraints (4). Empirically we adjust the cut-off for the singular values to 5 and set the initial weight λ for all quadrupole strengths to 10.

A problem is that the SVD solution provides both negative and positive focusing strengths, while the effect of the vertical impedance is always defocusing. For this reason, we iterate the SVD solution ten times; in each iteration we increase the weight λ by a factor 10, for those quadrupoles whose strengths were found to change in the wrong direction at the previous iteration step.

Figure 6 shows the current-dependent focusing obtained by this biased SVD analysis. For the 26-GeV/c data, large impedances are found at quadrupoles 11, 24, 88, 102, 139 and 164 (QD111, QDA119, QD307, QD319, QF420 and QD507), and for the more precise 14-GeV/c data, at quadrupoles 24, 80, 136, 140, 157, 164 and 236 (QDA119, QD301, QDA417, QD421, QD501, QD507 and QD635). The SPS regions 119 (near MKP kickers), 301–307 (arc?), 417–421 (near MKE kickers), and 507 (arc?) are identified at either energy as locations with high impedance.

Figure 7 compares the current-dependent phase changes predicted by the biased SVD fit with the measurements. For 26 GeV/c there is a fair agreement. At 14 GeV/c the measured phase changes agree perfectly with the SVD fit.

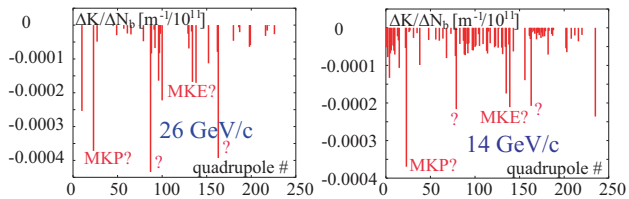

Figure 6: Impedance distribution obtained from SVD minimization at 26 GeV/c (left) and at 14 GeV/c (right); the singular-value cut-off was set to 5; the initial weight λ was 10 for all quadrupoles; it was increased by factors of 10 for strength changes ΔK of the wrong sign in 10 iterations.

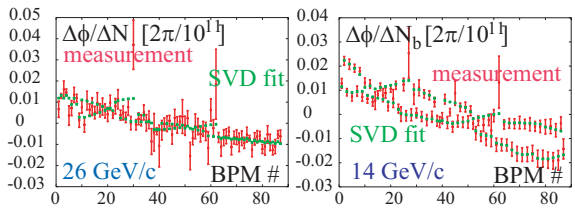

Figure 7: Current-dependent phase change predicted by SVD fit compared with the measurement at 26 GeV/c (left) and 14 GeV/c (right).

CONCLUSIONS

Our analysis suggests that most of the SPS transverse impedance is concentrated at a few locations of the ring. In addition to the regions of the MKP and MKE kickers, a large impedance also seems to exist in two arc locations, namely around points 301–307 and 507.

REFERENCES

[1] H. Burkhardt, CERN APC Meeting, 3 October 2003.
[2] L. Vos, "The inductive Impedance of the SPS," CERN-AB-2003-088 (ABP).
[3] D. Brandt et al., "Measurement of Impedance Distributions and instability Thresholds in LEP," PAC 95 (1995).
[4] G. Arduini et al., "Measurements of the SPS Transverse Impedance in 2000," IEEE PAC2001 Chicago (2001)
[5] J. Borer et al., "Harmonic Analysis of Coherent Bunch Oscillations in LEP," EPAC'92 (1992).
[6] A. Chao, Physics of Collective Beam instabilities in High-Energy Accelerators, John Wiley, New York, 1993.